AFM Molecular Images during Tip-Induced Surface Modification on the (010) Surface of a KCP(Br) Single Crystal

Tatsuji Kawasaki,[†,‡] **Lei Jiang,**[†] **Tomokazu Iyoda,**[†,⊥] **Toshinari Araki,**[‡]
Kazuhito Hashimoto,[†,§] **and Akira Fujishima*,**[†,§]

*Kanagawa Academy of Science and Technology, 1583 Iiyama, Atsugi, Kanagawa 243-02, Japan, Tokyo Gas
Co., Ltd., 7-7 Suehiro-cho, 1-Chome, Tsurumi-ku, Yokohama, Kanagawa 230, Japan, and Department of
Applied Chemistry, Faculty of Engineering, University of Tokyo, Hongo, Bunkyo-ku, Tokyo 113, Japan*

Received: August 30, 1996; In Final Form: December 17, 1996[⊗]

Molecular-resolution images of an electrochemically prepared single crystal of potassium tetracyanoplatinate
bromide complex (KCP(Br)) were recorded by atomic force microscopy during a tip-induced surface-
modification process in which the probing tip scraped off the topmost surface layer by layer. Two kinds of
molecular images on the (010) face of the KCP(Br) crystal correspond to alternate layered structures consisting
of tetracyanoplatinate layers and interstitial ions. One molecular arrangement was assigned to cyanide ligands
and interstitial K^+ and Br^- ions, in good agreement with that obtained from X-ray diffraction. The other
corresponds to rearranged interstitial ion (K^+ and Br^-) layer. The rearrangement of the interstitial ions during
the tip-induced surface modification involves both loss of half of the K^+ ions so as to preserve electroneutrality
of the surface and to stabilize the dislocations of the remaining ions. The present AFM imaging process
during the tip-induced surface modification provides mechanistic information on molecular and ionic
arrangements on the topmost surface.

Introduction

Scanning probe techniques such as scanning tunneling and
atomic force microscopies (STM and AFM) have become useful
tools to characterize[1−7] and fabricate nanoscale surface
structures.[8−12] There have been several reports on the mechan-
ical processing of crystal surfaces by STM and AFM. Typical
crystals, such as graphite, metal chalcogenides,[13] muscovite
mica,[14] and so on, have layered structures where individual
layers are stacked through van der Waals interaction. The
topmost surface layer of these crystals is easily stripped off by
tip-induced surface modification. The new surfaces exposed
during the surface modification are always atomically flat and
clean, so that a well-resolved molecular image may be acquired.
Until now, the number of suitable types of crystals for AFM
molecular imaging has been limited mostly due to unavoidable
tip-induced surface modification. There have also been few
studies of the image acquisition process itself. Detailed study
of tip-induced surface modification will provide significant
information concerning surface molecular rearrangements and
may lead to the possibility of obtaining depth-profile information
of layer-structured materials. In particular, inorganic semicon-
ductor superlattices and organic−inorganic heterostructures[15,16]
should be considered as target materials for the present approach.

The potassium tetracyanoplatinate bromide complex K_2Pt-
$[CN]_4 \cdot Br_{0.3} \cdot 3.2H_2O$, abbreviated KCP(Br), is a one-dimensional
(1D) conducting system that has been studied by many
researchers.[17−20] KCP(Br) exhibits needlelike crystals, and its
surfaces have chains running along the long axis of the
crystal.[17,21−23] The Pt−Pt distance along the column (2.89 Å)
is close to that in Pt metal (2.774 Å),[24,25] while the intercolumnar
Pt−Pt distance is larger (9.906 Å). This 1D structure results

in a large anisotropy of the electrical conductivity, where the
conductivity parallel to the Pt chains (*c* axis) is about 10^5 greater
than that perpendicular to the Pt chain direction (*a* and *b* axes).[23]
We have already reported that a molecular image of the (010)
surface of KCP(Br) was obtained using an attractive force of
10 nN in order to avoid surface modification.[26]

In this paper, we have examined the tip-induced surface-
modification process on the (010) face of the KCP(Br) single
crystal and have simultaneously collected high-resolution mo-
lecular images during the modification process. The molecular
arrangements and image acquisition process are described. The
tip-induced surface modification, familiar in AFM/STM studies
on molecular crystals, may be utilized to obtain atomically
resolved images of the topmost surface and the interstitial ions
in the vicinity of the surface of the crystal and, more importantly,
to understand molecular rearrangements on the freshly exposed
surface.

Experimental Section

Synthesis of KCP(Br) Single Crystals. The KCP(Br) single
crystals, $K_2Pt[CN]_4 \cdot Br_{0.3} \cdot 3.2H_2O$, were prepared by the elec-
trochemical method described previously.[27] An aqueous solu-
tion containing 0.723 mmol of potassium tetracyanoplatinate(II)
(Wako Pure Chemical Ind., Ltd.) in 2.4 mL of 1.0 mol/L KBr
(Wako Pure Chemical Ind., Ltd.) was placed in a 5 mL
electrolytic cell. An external voltage of 1.57 V was applied
between two Pt wire electrodes placed in the electrolytic cell at
11.6 °C. Copper-colored needle crystals grew on the Pt anode
predominantly in a direction normal to the surface, e.g., up to
a size of 7 mm × 2 mm × 1 mm within 12 h electrolysis. The
crystallographic parameters of the KCP(Br) crystals prepared
here were $a = b = 9.906$ Å and $c = 5.783$ Å, based on X-ray
powder diffraction, with peak assignments reported previously,
as shown in Figure 1. Prior to the AFM measurements, the
crystals were stored at 23 °C under a controlled relative humidity

---

† Kanagawa Academy of Science and Technology.
‡ Tokyo Gas Co.
§ University of Tokyo.
⊥ Present address: Department of Industrial Chemistry, Faculty of
Engineering, Tokyo Metropolitan University, 1-1 Minami-Osawa Hachioji,
Tokyo 192-03, Japan.

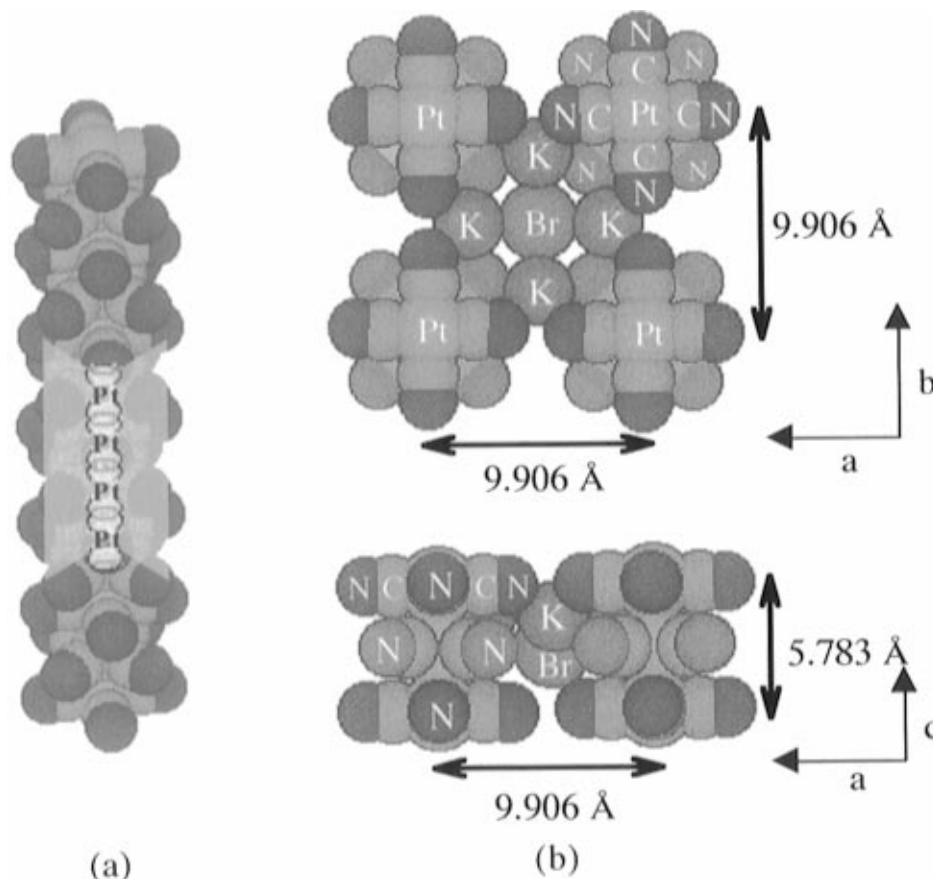**Figure 1.** Molecular arrangement of a single crystal of potassium tetracyanoplatinate bromide complex $K_2Pt[CN]_4 \cdot Br_{0.3} \cdot 3.2H_2O$, abbreviated KCP-(Br). (a) A columnar structure consisting of staggered tetracyanoplatinate units with 45° of torsion angle along the Pt–Pt bond. (b) Molecular arrangement of the unit cell of the monoclinic crystal (space group *P4mm*), $a = b = 9.906$ Å and $c = 5.783$ Å. Water molecules are omitted for clarity.

of 72% over a saturated aqueous solution of NH_4Cl and KNO_3 (Wako Pure Chemical Ind., Ltd.).[28] Without any further treatment, the needle crystals were mounted on the AFM stage with the mirrorlike (010) surface facing up.

AFM Measurements. An SPA3000 AFM (Seiko Instruments) was used under ambient atmosphere at 23 °C and about 70% relative humidity, using a Si_3N_4-coated cantilever (100 μm tripod, Seiko Instruments) and a 20 μm piezoelectric tube scanner. We have found that high-resolution images can be obtained using an appropriate repulsive force (21 pN) in the case of molecular crystals such as KCP(Br). The AFM measurements were performed in a constant height mode at scan rates ranging from 8.12 to 16.28 Hz. The height information was simultaneously obtained from topographic imaging. For the *x* and *y* directions, the piezoelectric tube scanner was calibrated by imaging a freshly cleaved surface of a mica for each series of measurements. To minimize thermal drift and electrical fluctuations of the power supply, the AFM instrument was allowed to stabilize before the measurements. Some images were low-pass filtered (1 kHz) to enhance the corrugation features of the surface. By collecting images of different scanning directions and at different magnifications, we ensured that the observed structures were real and self-consistent.

Results and Discussion

KCP(Br) Surface Topography. Figure 2 shows a large scale image of one of the mirrorlike faces of the KCP(Br) needle crystal using a 10 nN attractive force (800 nm × 600 nm). The observed face exhibited extremely flat terraces with several steps. Each step height was 10.3 ± 0.6 Å, which is consistent

with the crystallographic parameters for the *a* and *b* axes (9.906 Å). Therefore, the observed face may be assigned to the (010) face, with atomically flat terraces and monolayer steps.

We have proposed that this morphology is the result of a layer-by-layer growth process,[26] which is attributed to the anisotropic electronic conductivity. During electrocrystallization, it is supposed that the reactant $[Pt^{II}(CN)_4]^{2-}$ is oxidized to $[Pt^{IV}(CN)_4Br_2]^{2-}$ through redox mediation by electrogenerated Br_2 near the anode. The reactant and the resulting products crystallize on the anode to form a mixed-valence crystal. High conductivity along the columns plays a significant role in the crystal growth. The layer edges function as molecular level electrodes in the redox process and therefore act as growth sites. On the contrary, low conductivity along the *a* and *b* axes completely supresses the redox process on the terraces, which are therefore atomically flat, with no domains and no nuclei. No interstitial ions, K^+ and Br^-, were found on this surface.

The image shown in Figure 2a was taken after small scale images (6 nm × 6 nm) were collected in three different regions within this large scale area. Here, a brief discussion is required concerning the three holes shown in Figure 2a, which were traces left by AFM tip after the small scale scanning, i.e., the surface-modification procedure described here. It should be note that neither pit nor hillock was observed in this large area prior to the surface-modification process during the small-scale scanning. As the tip approached the surface with increasing atomic force between tip and sample, it was observed that the scanning tip stripped away the topmost surface layer to expose the underlying layer. This stripping process may be regarded as a type of tip-induced surface modification process. Therefore,
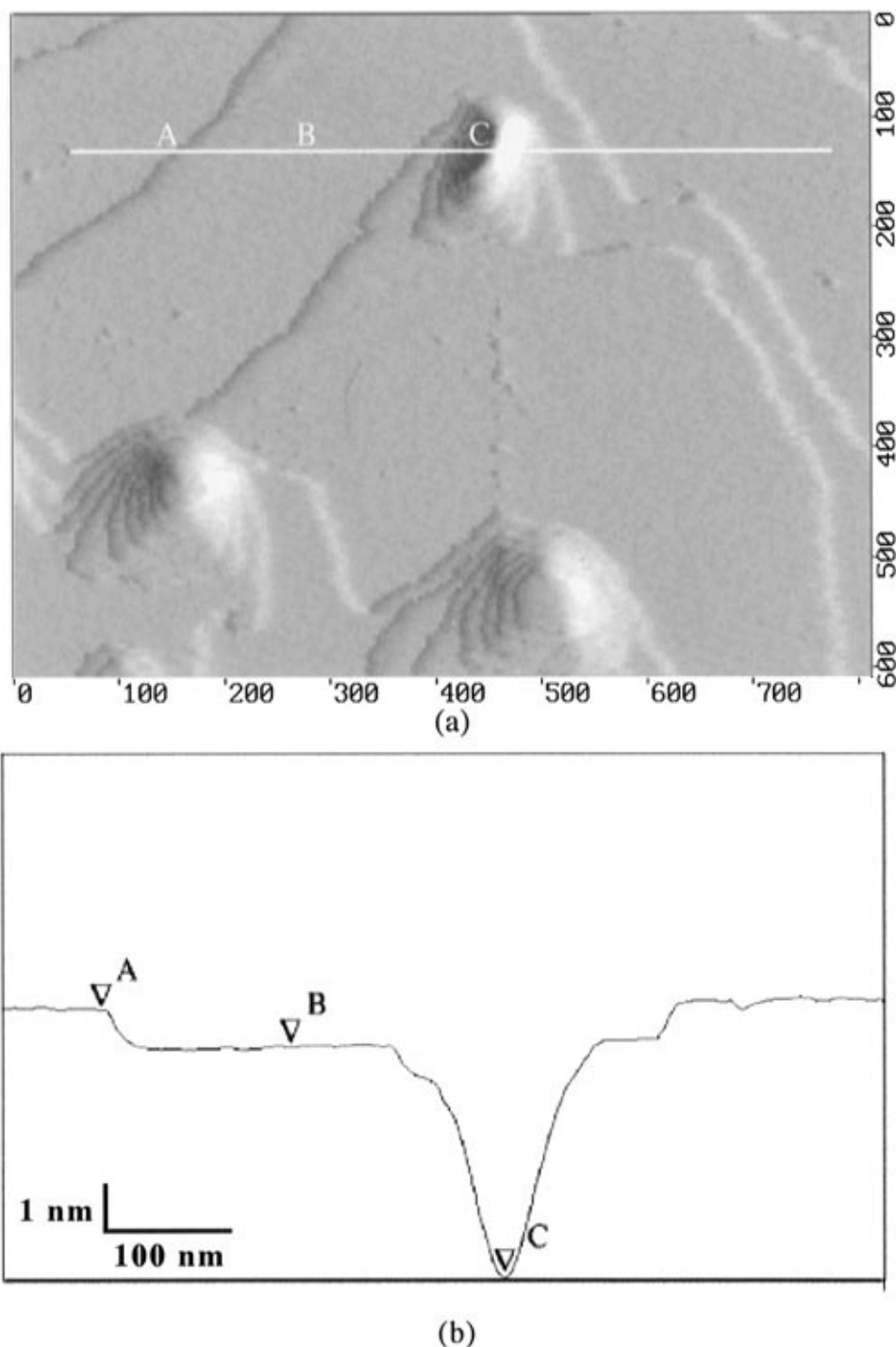
The (010) Surface of a KCP(Br) Single Crystal

J. Phys. Chem. B, Vol. 101, No. 14, 1997 **2725**

Figure 2. (a) Large-scale AFM image (800 nm × 600 nm) of the (010) face of KCP(Br). All of the step heights of the observed terraces are 10.3 ± 0.6 Å, which is consistent with the crystallographic parameter for the *a* or *b* axis (9.906 Å). The three holes in the inset resulted from the surface modification, as is described in the text. Individual step heights observed in the holes are also 10.3 ± 0.6 Å, corresponding to the thickness of the monolayers. (b) Vertical profile along the white straight line in (a).

these large holes were produced during surface modification at three separate locations (6 nm × 6 nm). The structures of the multiple steps were clearly observed in these holes. Figure 2b shows a vertical profile along the white line in Figure 2a. The step height (A−B) was 10.3 ± 0.6 Å, corresponding to the molecular thickness, i.e., the crystallographic parameter by the *a* and *b* axes. A terraced structure with several monolayer steps was observed in these holes. This observation indicates that the surface layer was scraped off layer by layer during the modification process.

Molecular Images of KCP(Br). In the AFM measurements, two types of molecular images were observed on the (010) face

of the KCP(Br) crystal during the surface modification, which was carried out using a 21 pN of repulsive force. Figure 3a shows a molecular-resolution AFM image (5 nm × 5 nm) in the constant height imaging mode.[29] There are several long parallel columnar structures. The direction of the columnar structures corresponds to the long axis of the crystal mounted on the scanner table, so that the [001] direction can be assigned. The molecular arrangement and even the internal atomic arrangement can be observed in the image. Along the columns, there are bright spots in the regular rhomboid arrangement, labeled 1 and 2 in the image. The lengths of the diagonal lines are 6.22 ± 0.44 and 4.15 ± 0.36 Å. The rhombus appears to
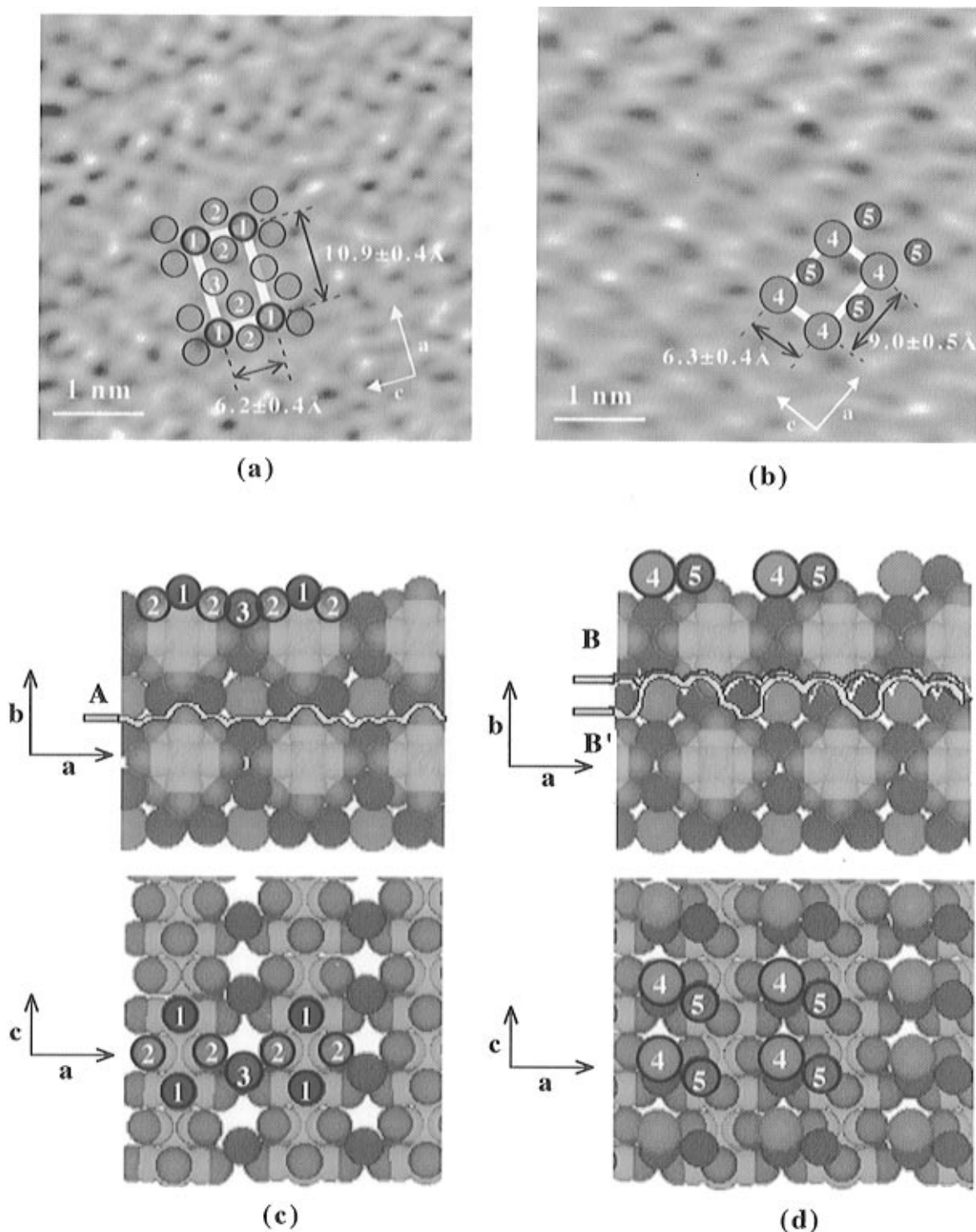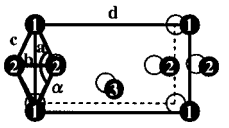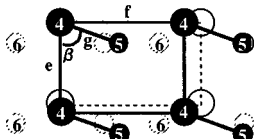
Figure 3. Molecular-resolution AFM images of the (010) surface of the KCP(Br) crystal. (a) The bright rhombically shaped spots and the dim spots between the columns are assigned to the protruding N atoms and the interstitial K^+ ions, respectively. (b) The bright and the dim spots in the image are assigned to the Br^- and K^+ on the surface, respectively. (c) Top and side views of the space filling model on the (010) face of KCP(Br) based on X-ray crystallographic data. Atoms **1** and **2** are the most protruding N atoms of the cyanide ligands and the second furthest protruding N atoms of the neighboring cyanide ligands (0.92 Å lower), respectively. Atom **3** is interstitial K^+ on this face. (d) Top and side views of the space filling model of arrangement II, which is constructed from the AFM image in Figure 3b. Atoms **4** and **5** are interstitial Br^- and K^+, respectively.

be 3.76 ± 0.3 Å on the sides and has an obtuse included angle of 107.9 ± 5.8°. The distance between the columns was 10.83 ± 0.45 Å. Dim spots are arranged periodically in the spaces between the columns. We identified the individual spots in this image, compared with the space filling model (Figure 3c) constructed from the X-ray diffraction data.[25] Atoms 1 and 2 denoted in Figure 3c are the furthest protruding nitrogen (N) atoms of the cyanide ligands on the (010) face and the second

furthest protruding N atoms of the neighboring cyanide ligands, which are 0.92 Å lower than the furthest protruding N atoms on the (010) face, respectively. Atom 3 is an interstitial potassium cation (K^+) on this face. Along the column, the N atoms are arranged in a regular rhomboid shape. The longer diagonal line is 5.783 Å (crystallographic parameter c) and the shorter one is 4.56 Å. The side length is 3.67 Å and the obtuse included angle is 100.24°. The length between the columns is

The (010) Surface of a KCP(Br) Single Crystal

J. Phys. Chem. B, Vol. 101, No. 14, 1997 **2727**

TABLE 1: Internal Atomic Arrangements in the (010) Face of the KCP(Br) Single Crystal[a]

Atomic arrangement in the (010) face		parameter	AFM images on the (010) face	X-ray diffraction on the single crystal[25]
I Fig. 3a		a	6.22 ± 0.44 Å	5.783 Å
		b	4.15 ± 0.36 Å	4.56 Å
		c	3.76 ± 0.30 Å	3.67 Å
		d	10.83 ± 0.45 Å	9.906 Å
		α	107.9 ± 5.8°	100.24°
II Fig. 3b		e	6.3 ± 0.4 Å	5.783 Å
		f	9.0 ± 0.5 Å	9.906 Å
		g	4.2 ± 0.4 Å	3.35 Å
		β	70.3 ± 2.8°	64.88°

[a] The closed and open circles show atomic arrangements of relatively protruded atoms on the (010) face which are obtained from X-ray crystallographic data and the present AFM image, respectively. Atom 1: the most protruded nitrogen (N) atoms of the cyanide ligands of the (010) face. Atom 2: the second protruded N atoms of the neighboring cyanide ligands that were about 0.92 Å lower than the most protruded N atoms on the (010) face. Atom 3: an interstitial potassium cation (K$^+$) on this face. Atoms 4: interstitial Br$^-$. Atoms 5 and 6: interstitial K$^+$, one of them in the unit arrangement is lost in the surface reconstruction. Atom 6 is missing alternatively in Figure 3b. Both atomic arrangements I and II, are observed in Figure 3a,b, respectively.

9.906 Å (crystallographic parameters, $a = b$). Table 1 summarizes the structural parameters obtained from the present AFM images, with reference to the X-ray crystallographic data. Both sets of the parameters are reasonably consistent. The bright rhombically arranged spots and the dim spots between the columns can be assigned to the protruding N atoms and the interstitial K$^+$ ions, respectively.

Figure 3b shows another molecular AFM image. The rectangle, formed by the bright spots, is 9.0 ± 0.5 Å by 6.3 ± 0.4 Å, close to the crystallographic parameters for the a and c axes of the bulk KCP(Br) crystal. Small dim spots are found between the line connecting the bright spots along the c axis. The arrangement II of these spots is completely different from arrangement I. There are no spots that correspond to atom 2 in Figure 3a. Moreover, the bright spots appear larger than the spots assigned to the protruding N atoms in Figure 3a. Considering the image spot size predicted from the ionic radii, bromide ions (Br$^-$) are the largest ions among the elements that comprise KCP(Br). These results imply that the observed face is the topmost surface, with interstitial K$^+$ and Br$^-$ left on the second layer, as shown in arrangement I. The two space-filling models in Figure 3d are the top and the side views of arrangement II which is constructed from the AFM image in Figure 3b. Atoms **4** and **5** are interstitial Br$^-$ and K$^+$, respectively, in Figure 3d. The bright and dim spots are consistent with the Br$^-$ and K$^+$ arrangement of the bulk structure shown in Table 1. Although atoms **6**, as shown by the dashed circles in Table 1, should exist on the same face, considering the bulk structure based on X-ray analysis, these atoms are missing alternately in Figure 3b. The combined evidence of the missing atoms **6** and the dislocations of the other interstitial ions lead us to consider a surface reconstruction during the surface modification, which will be discussed in the following section.

Thus, two kinds of AFM images suggest that the topmost molecular layer on the (010) face of KCP(Br) crystal tends to be stripped off to a specific depth that reflects the interlayer interaction forces between columns and the local mechanical stress applied by the scanning tip.

Acquisition Process of Molecular-Resolution Images. We have observed a striking contrast in the acquisition process of the two types of molecular images shown in Figure 3a,b. It is worthwhile, even phenomenologically, to describe the acquisition processes of these images and hopefully to examine the simultaneous rearrangement of a surface that is freshly exposed during the surface modification with the AFM tip.

In the case of the image shown in Figure 3a, molecular images were occasionally obtained within a series of less-resolved images and were realized only for a while but long enough to acquire the image. In the early stages of the AFM imaging, a disordered molecular image (Figure 4a) was obtained, and then changed to a series of ordered molecular images (Figure 4b–d), which were sequentially collected for every image acquisition. Even the less-resolved images (Figure 4b,d) allow one to visualize the outline of molecular arrangement I. However, it should be emphasized here that the well-resolved image (Figure 4c) reveals a clear molecular structure with the internal atomic arrangement I which agrees with that expected from the bulk KCP(Br) crystal. On the contrary, the well-resolved image in Figure 3b was relatively stable during the acqusition of a number of images. The image of Figure 4f was obtained six imaging cycles after the image in Figure 4e was acquired. Both images show almost the same molecular arrangements, with little trace of surface modification. It should be noted that both images (Figure 3a,b) were acquired under the same AFM operating conditions. This implies that the two types of surface arrangement have different mechanical stabilities with respect to the surface-modification process.

A specific surface reconstruction involving the interstitial ions, K$^+$ and Br$^-$, may be introduced to explain the relatively stable arrangement II shown in Figure 3b. The arrangement of K$^+$ and Br$^-$ ions expected from X-ray crystallographic data is shown by the white circles in arrangement II in Table 1. Atoms **6** consist of the interstitial K$^+$ ions which remain after half are lost so as to preserve electroneutrality of the new topmost surface during the tip-induced surface-modification process. The ions remaining on the surface may then rearrange to the energetically stable arrangement II, as shown in Figure 3b.

During surface modification, there are two possible ways in which the AFM tip strips away the topmost layer with or without the interstitial ions, routes A and B, as shown in Figure 3c,d, respectively. Arrangement I appears after surface modification via route A. The other modification, via route B, is accompanied by a surface rearrangement in which the interstitial K$^+$ ions are lost alternately, so that arrangement II is observed. Consequently, the surface modification appears to proceed via route B′ in Figure 3c. It has been reported that there are three types of crystal water molecules[30,31] coordinating to the cyanide ligand and the interstitial ions through hydrogen bonding and ion–dipole interactions, based on the thermogravinometric measurements.[32] The crystal water should play a significant role in stabilizing the atomic arrangements in the KCP(Br), so that a delicate balance between the various types of interactions involving the water molecules may be responsible for the selection between the two routes via which the scanning tip scrapes off the topmost layer.

Conclusion

Two types of molecular images were obtained on the (010) surface of the KCP(Br) single crystals during the tip-induced surface modification process, in which the scanning AFM tip scraped off the topmost surface layer by layer. The molecular
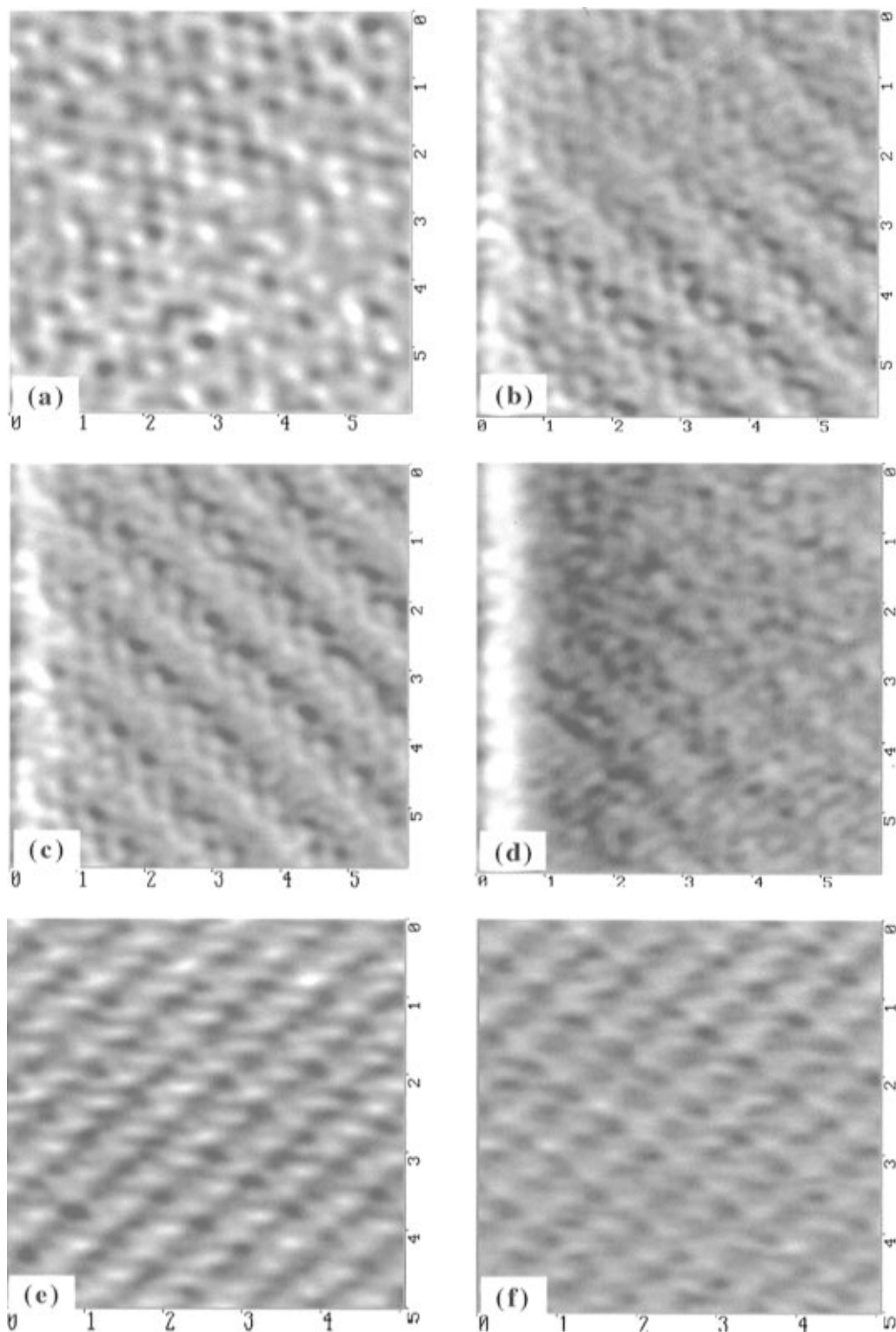
Figure 4. Sequential image acquisition during surface modification on the (010) face of KCP(Br). All of the images were obtained by scanning the 6 nm × 6 nm area shown. Images a–d correspond to arrangement I. (a) Disordered molecular images were obtained in the early stages of the AFM imaging. (b–d) A series of images was sequentially obtained at every single image acquisition after that shown in Figure 4a. Images e and f correspond to arrangement II. (e) This image was obtained in the early stages of AFM imaging. (f) This image was obtained after six image acquisitions subsequent to that shown in e.

arrangement in one type of image was in good agreement with that for the (010) face consistent with the bulk structure obtained by X-ray diffraction. The arrangement in the second type of image was interpreted in terms of the simultaneous surface rearrangement of the interstitial ions, K^+ and Br^-. The image acquisition process during tip-induced surface modification is strongly influenced by the stability of the topmost molecular arrangements. Further experiments will be required to optimize

the operating conditions for the AFM tip to strip off the topmost layer. During the tip-induced surface modification that is always encountered in AFM/STM studies of mechanically weak molecular crystals, the image acquisition process occasionally will provide information on local mechanical properties through a force analysis, as well as simultaneous surface rearrangements, leading to the possibility of dynamic imaging on the surface in question. Additionally, the imaging techniques reported here

will help to open up the new field of molecular-resolved depth profiling via surface modification with the possibility of obtaining three-dimensional structural analyses, as in tomography, by computed reconstruction of the structure from images collected during the modification process.

References and Notes

(1) Dagata, J. A.; Tseng, W.; Bennett, J.; Dobisz, E. A.; Schneir, J.; Harary, H. H. *J. Vac. Sci. Technol.* **1992**, *A10(4)*, 2105.
(2) Hillier, A. C.; Ward, M. D. *Science* **1994**, *265*, 1261.
(3) Schott, J. H.; Yip, C. M.; Ward, M. D. *Langmuir* **1995**, *11*, 177.
(4) Magonov, S. N.; Whangbo, M. H. *Adv. Mater.* **1994**, *6*, 355.
(5) Magonov, S. N.; Bar, G.; Gorenberg, A. Y.; Yagubskii, E. B.; Cantow, H. J. *Adv. Mater.* **1993**, *5*, 453.
(6) Scott, G. B.; Johnson, S. R.; Swanson, B. I.; Ren, J.; Whangbo, M. H. *Chem. Mater.* **1995**, *7*, 391.
(7) Louder, D. R.; Parkinson, B. A. *Anal. Chem.* **1994**, *66*, 84.
(8) Corbitt, T. S.; Crooks, R. M.; Ross, C. B.; Hampden-Smith, M. J.; Schoer, J. K. *Adv. Mater.* **1993**, *5*, 935.
(9) Parkinson, B. A. *J. Am. Chem. Soc.* **1990**, *112*, 7498.
(10) Avouris, P. *Acc. Chem. Res.* **1995**, *28*, 95.
(11) Bengel, H.; Cantow, H. J.; Magonov, S. N.; Whangbo, M. *Adv. Mater.* **1995**, *7*, 483.
(12) Leung, O. M.; Goh, M. C. *Science* **1992**, *255*, 64.
(13) Delawski, E.; Parkinson, B. A. *J. Am. Chem. Soc.* **1992**, *114*, 1661.
(14) Miyake, S. *Appl. Phys. Lett.* **1995**, *67(20)*, 2925.
(15) Takada, J.; Awaji, H.; Koshioka, M.; Nakajima, A.; Nevin, W. A. *Appl. Phys. Lett.* **1992**, *61*, 2185.
(16) Kimizuka, N.; Kunitake, T. *Adv. Mater.* **1996**, *8*, 89.
(17) Keller, H. J. In *In Extended Linear Chain Compounds*; Miller, J. S., Ed.; Plenum: New York, 1982; Vol. 1.
(18) Shchegolev, I. F. *Phys. Status Solidi A* **1972**, *12*, 9.
(19) Miller, J. S. *Science* **1976**, *193*, 189.
(20) Rice, M. J. *Phys. Bull.* **1975**, *26*, 493.
(21) Krogmann, K. *Angew. Chem., Int. Ed. Engl.* **1969**, *8*, 35.
(22) Bernasconi, J.; Bruesch, P.; Zeller, H. R. *J. Phys. Chem. Solids* **1974**, *35*,
(23) Zeller, H. R.; Beck, A. J. *J. Phys. Chem. Solids* **1974**, *35*, 77.
(24) In *CRC Handbook of Chemistry and Physics*; 57th ed.; CRC Press, Inc.: Cleveland, OH, 1995.
(25) Peters, C.; Eagen, C. F. *Inorg. Chem.* **1976**, *15*, 782.
(26) Kawasaki, T.; Jiang, L.; Iyoda, T.; Araki, T.; Tryk, D. A.; Hashimoto, K.; Fujishima, A. *Chem. Lett.* **1995**, *10*, 879.
(27) Miller, J. S. In *Inorg. Synth.*; Shriver, D. F., Ed.; Wiley: New York, 1979; Vol. 19, p 13.
(28) Kuse, D.; Zeller, H. R. *Solid State Commun.* **1972**, *11*, 355.
(29) We routinely confirm the validity of the surface structures observed in all of the images by collection of images in different scanning directions and at different magnifications. For example, the image in Figure 4c was taken when the sample was rotated 60° clockwise after the image in Figure 3a was collected. The important point is to obtain a consistent rhombic arrangement of bright spots in both images, regardless of the scanning direction. The different arrangement in Figure 3b is quite obvious, so that the discussion on the different arrangements is valid.
(30) Masin, F.; Leo, V. *Solid State Commun.* **1982**, *43*, 61.
(31) Whitney, J. R.; Billoski, T. V.; Jones, V. R. In *New Directions in Paleontology*; Billoski, T. V., Ed.; Academic Press: New York, 1987; p 24.
(32) Peters, C.; Eagen, C. F. *Phy. Rev. Lett.* **1975**, *34*, 1132.